Mass Transfer from Spheroids to an Air Stream

A. H. P. SKELLAND and A. R. H. CORNISH

Illinois Institute of Technology, Chicago, Illinois

In recent years several investigators have studied heat and mass transfer rates from spheres, hemispheres, cylinders, slabs, cubes, and disks (*1, 5, 6, 7, 13, 19, 20, 21, 24, 27*). Very little effort however has been directed towards the study of transfer processes from other shapes such as spheroids. A literature survey shows that the spheroid may be regarded as an idealized shape in many mass transfer operations when one phase is dispersed in the other (*8, 15, 16, 17, 18*).

In liquid-liquid extraction for example droplets of the disperse phase may approximate internally stagnant, nonoscillating oblate spheroids, due to a particular combination of physical properties or to the presence of trace quantities of surface active impurities (*9, 11, 12*).

At a given Reynolds number spheroids of different major to minor axis ratios (eccentricities) are subject to drag forces of different magnitudes (*15, 22, 25*). This may be regarded as a qualitative indication that mass transfer rates in the continuous phase are also substantially dependent upon eccentricity. In the present work this question has been explored by suspending oblate naphthalene spheroids in an air stream over a Reynolds number range of 130 to 6,000; eccentricities varied from 1:1 to 3:1.

These findings should contribute towards the ultimate objective of the design of extraction columns from rate relationships, without the need for experimentally determined efficiencies. The detailed procedure is to be published later.

THEORETICAL CONSIDERATIONS

Frössling (*7*) showed theoretically that for nonangular bodies of revolution with their axes parallel to the direction of flow the local values of the Sherwood number are proportional to the square root of the Reynolds number; this result was demonstrated theoretically for the region between the front stagnation point and the separation point. Theoretical predictions are lacking beyond the separation point. Frössling also showed that for the limiting case of very large Schmidt numbers the Sherwood number is exactly proportional to the cube root of the Schmidt number. For other ranges of the Schmidt number he was able to show theoretically that the quantity $N_{Sh}/(N_{Re})^{1/2}(N_{Sc})^{1/3}$ remains approximately constant.

Further evidence for anticipating that N_{Sh} will be related to $(N_{Re})^{1/2}$ and to $(N_{Sc})^{1/3}$ in forced convection is provided by other experimental work on a wide variety of shapes (*1, 6, 13, 20, 24, 27*).

Several workers have correlated N_{Sh} by direct addition of terms representing transfer by purely molecular diffusion and by forced convection (*6, 13, 27, 28*). A similar number of workers have omitted the term for transfer by purely molecular diffusion from the correlation (*5, 19, 20, 21, 31*). Because the direct additivity of these two effects is open to question, correlations of the present data were obtained with and without the term for transfer by purely molecular diffusion, and the results were compared in an attempt to resolve this issue.

At low values of N_{Re} free convection also contributes to the rate of mass transfer. Garner and Keey (*10*) showed that for spheres free convection effects are negligible when the Reynolds number exceeds the limiting value

$$N_{Re} > 0.4\,(N'_{Gr})^{1/2}\,(N_{Sc})^{-1/6} \quad (1)$$

For the 1-in. spheres in the present work Equation (1) indicates that natural convection effects are negligible at $N_{Re} > 15$.

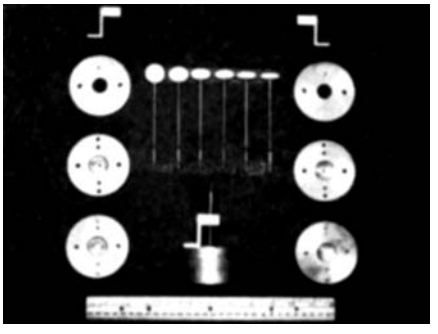

Fig. 1. Samples of the spheroids and molds used in this work.

Various workers (*2, 21*) have found that the intensity of turbulence of the continuous phase can substantially increase the rates of transfer. Turbulence measurements with a hot-wire anemometer showed that, according to the findings of Brown, Sato, and Sage (*2*), the rates of transfer in the present work were not increased because of turbulence by more than about 2%.

It is expected from the above considerations that the data will be correlated by one of the following relationships:

1. Without the term for transfer by purely molecular diffusion:

$$N_{Sh} = C_1(N_{Re})^{m_1}\,(N_{Sc})^{1/3} \quad (2)$$

2. With the term for transfer by purely molecular diffusion:

$$N_{Sh} = N_{Sh_o} + C_2(N_{Re})^{m_2}\,(N_{Sc})^{1/3} \quad (3)$$

m_1 and m_2 are expected to be approximately ½. N_{Sh_o} is the Sherwood number when molecular diffusion is the only transfer mechanism.

The Reynolds and Sherwood numbers both contain a characteristic dimension representing the geometry of the body; correct definition of this dimension may render C_1 and C_2 independent of eccentricity. Some of the characteristic dimensions (D_c) which have previously been used with success are as follows:

1. The diameter of a sphere of the same volume as the body (D_1).
2. The length of the minor axis of the body (D_2).
3. The total surface area of the body divided by the perimeter normal to flow (D_3).
4. The diameter of a sphere of the same surface area as the body (D_4).
5. The average of the axes parallel and normal to flow (D_5).
6. The sphericity multiplied by the diameter of a sphere of the same volume as the body (D_6).
7. The axis normal to flow (D_7).

To facilitate correlation Equations (2) and (3) were rearranged as follows:

$$j_D = \frac{N_{Sh}}{(N_{Re})\,(N_{Sc})^{1/3}} = C_1(N_{Re})^{n_1} \quad (4)$$

$$j'_D = \frac{N_{Sh} - N_{Sh_o}}{(N_{Re})\,(N_{Sc})^{1/3}} = C_2(N_{Re})^{n_2} \quad (5)$$

where the left-hand sides of Equations (4) and (5) are independent of the

Tabular material has been deposited as document number 7355 with the American Documentation Institute, Photoduplication Service, Library of Congress, Washingon 25, D. C., and may be obtained for $3.75 for photoprints or for $2.00 for 35-mm. microfilm.

A. H. P. Skelland is with the University of Notre Dame, Notre Dame, Indiana. A. R. H. Cornish is at Imperial College, The University of London, London, England.

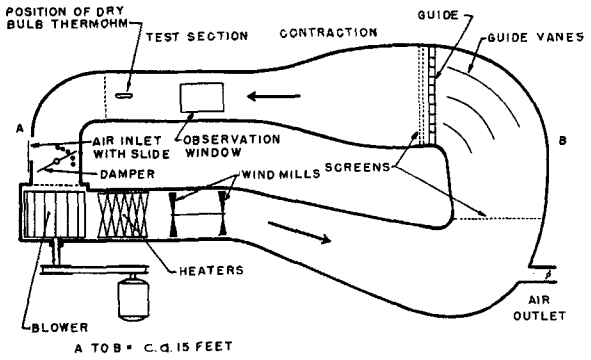

Fig. 2. Diagram of wind tunnel.

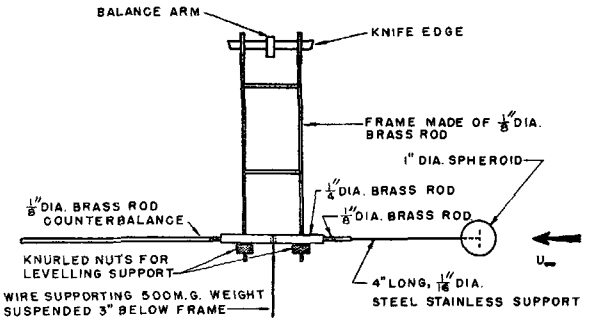

Fig. 3. Sketch of spheroid support assembly.

characteristic dimension, provided that k_c is based on the actual surface areas of the bodies.

A further form of correlation was examined, with the use of D_1 and with k_c based on the area of a sphere with the same volume as the body. The corresponding left-hand sides of Equations (4) and (5) were in this case denoted by j_{D_S} and j'_{D_S}, respectively.

For a mechanism of purely molecular diffusion from oblate spheroids the following relationship has been derived (32):

$$\frac{k_c}{D_V} = \frac{N_{Sh_o}}{D_c} = \frac{\left(\frac{c}{(c_B)_{1.m}}\right)[4\pi(d^2-f^2)^{1/2}]}{\left[\frac{\pi}{2} - \tan^{-1}\left(\frac{f^2}{d^2-f^2}\right)^{1/2}\right]\left[2\pi d^2 + \frac{\pi f^2 d}{(d^2-f^2)^{1/2}} \ln\left\{\frac{d+(d^2-f^2)^{1/2}}{d-(d^2-f^2)^{1/2}}\right\}\right]} \quad (6)$$

For a sphere this reduces to the well-known expression

$$N_{Sh_o} = 2\frac{c}{(c_B)_{1.m}} \quad (7)$$

and for a disk, where D_c is the disk diameter, one obtains

$$N_{Sh_o} = \frac{8}{\pi}\frac{c}{(c_B)_{1.m}} \quad (8)$$

APPARATUS AND TECHNIQUES

Spheroids

Oblate naphthalene spheroids of eccentricities 1:1 (sphere), 5:4, 5:3, 2:1, 5:2, and 3:1, each having a major axis length of 1 in., were made by casting reagent-grade naphthalene in brass molds. Representative samples of the spheroids and molds are shown in Figure 1. The supports were of stainless steel, 1/16 in. in diameter and 4 in. long. To make the spheroids molten naphthalene at 90°C. was injected into the preheated molds with a hypodermic syringe, the needle of which extended to the bottom of the cavity. To prevent voids forming within the spheroids during cooling the molds were cooled slowly from the bottom upwards, so that the molten naphthalene in the reservoir could flow down into the cavity. (The ¾-in. diameter hole in the upper plate, Figure 1, constituted this reservoir.)

The molds were placed on a cool metal plate to promote solidification in the cavity, while a hot metal plate just above the molds delayed solidification in the reservoir. For the spheroids to separate cleanly from the molds it was essential for the solidification and subsequent cooling process to near room temperature to be carried out slowly (over a period of at least 3 hr.). By this procedure the contaminating effects associated with the use of mold release agents were avoided.

Wind Tunnel

The spheroids were suspended in the test section of the closed-circuit, insulated, wind tunnel shown diagrammatically in Figure 2. The tunnel was about 15 ft. in overall length, with a horizontal test section 15 in. in diameter and 30 in. in length. The test section was situated at the outlet from a contraction section (contraction ratio = 4.25:1) which provided a flat velocity profile, as shown by velocity traverses. Hot-wire anemometer measurements showed that screens of 28-mesh wire cloth at the entrance to the contraction section reduced turbulence to a low level. The difference between the static pressure in the tunnel and atmospheric pressure was less than 0.05 mm. Hg in all cases. The air temperature in the tunnel was maintained constant in each run, at a magnitude near 50°C. Temperatures were measured at intervals during the runs by three thermocouples located 2 in. from the spheroids and in the same vertical plane. Velocities were measured before and after each run with a hot-wire anemometer. The point of measurement was that occupied by the spheroid during the run; velocities ranged from 0.5 to 14.1 ft./sec. The spheroids were suspended in the wind tunnel by the support shown in Figure 3. This support was in turn suspended from the knife edge of the balance arm of a continuous weighing device (23). Interpretation of the charts produced by this device showed that the rate of mass transfer remained constant throughout each run. The precise amount transferred in each run was therefore determined by initial and final weighings.

Measurements of enlarged shadow photographs taken of the spheroids before and after each run showed that the average change in eccentricities was 2.5% and the average change in the major axes was 1.3%. The average loss in mass of the spheroids was 8.6%.

Experimental Procedure

Before each run the spheroids were photographed and weighed and replaced in the molds; the reservoir and feed channel were then filled with powdered naphthalene to avoid premature sublimation losses. This assembly was then preheated in a controlled oven to a temperature 2 deg. below that of the air stream. The maximum loss of naphthalene incurred in this procedure was found from thirteen runs to be 0.0029 g. A 2.2°C. difference between the air and spheroid temperatures was the average difference found in eight runs in which thermocouples were embedded at various positions in the spheroids.

The preheated spheroid was removed from the mold inside the test section and attached to the support while shielded from the air stream. The run was started on removal of the shield.

At the end of each run the spheroid was removed from the air stream and weighed at recorded intervals. The mass of the spheroid on removal from the test section was then obtained by extrapolation of these weighings. The spheroid was photographed at the end of these final weighings.

Physical Properties

Air densities were calculated in accordance with the ideal gas law;

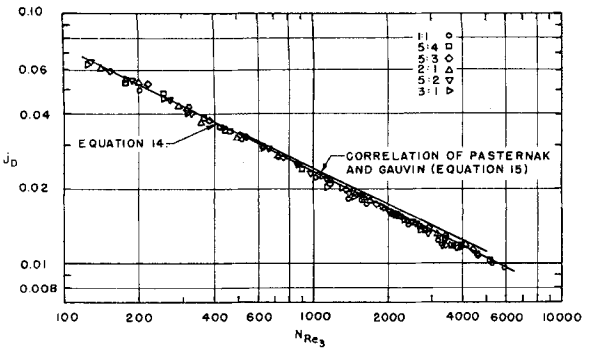

Fig. 4. Plot of j_D vs. N_{Re_3}.

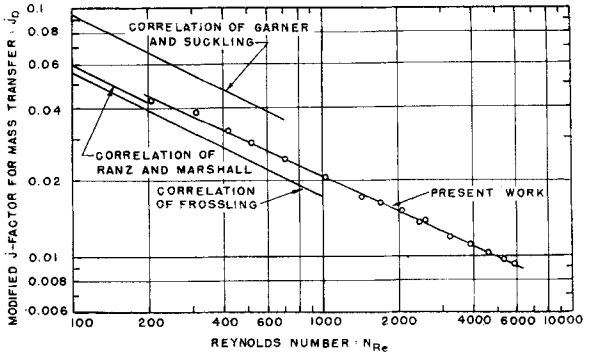

Fig. 6. Comparison of the data obtained for spheres with correlations obtained by other workers.

viscosities of air were calculated by means of Sutherland's formula (*26*). In the absence of experimental data the diffusion coefficient for napthalene vapor diffusing through air was calculated with Gilliland's semiempirical correlation (*14*).

The vapor pressure of naphthalene was calculated from the expression presented by Uno (*29*):

$$\log_{10} P^+ = 11.84528 - \frac{3{,}857}{T} \quad (9)$$

P^+ is in mm. Hg, and T is in °K.

Densities, viscosities, and diffusivities were calculated at the mean film temperature and saturation vapor pressures at the estimated surface temperature (air temperature minus 2.2°C.).

Calculation of k_o

The mass transfer coefficient k_c was calculated for each run from the expression

$$N = \frac{k_c}{RT}(P^+ - P_o)\,A \quad (10)$$

To maintain P_o at a low level throughout each run part of the air stream was removed from the tunnel at a measured rate at the outlet vent shown in Figure 2. This was replaced by fresh air entering at the inlet vent and by naphthalene subliming at the measured rate from the spheroid. A naphthalene balance on these streams showed that P_o was always less than $0.004P^+$ and therefore was regarded as zero. In Equation (10) T is the absolute mean film temperature.

In accordance with the definitions of j_{D_s} and j'_{D_s} given above

$$j_{D_s} = j_D \frac{1}{\psi} \quad (11)$$

$$j'_{D_s} = j'_D \frac{1}{\psi} \quad (12)$$

Results

Plots on logarithmic co-ordinates were made of j_D and j'_D vs. N_{Re_1} to N_{Re_7}, where N_{Re_1} to N_{Re_7} are Reynolds numbers calculated with D_1 to D_7, respectively. Further plots were made of j_{D_s} and j'_{D_s} vs. N_{Re_1}.

Inspection of these plots revealed that the best correlations were clearly those of j_D and j'_D vs. N_{Re_3}, so statistical treatment was restricted to these two forms. [N_{Re_3} is based on D_3, the characteristic dimension proposed by Pasternak and Gauvin (*24*).]

The data were fitted by means of a generalized linear/nonlinear least squares procedure programmed for an IBM-650 digital computer by Bukacek (*3, 4*). In the first instance the data were fitted so as to minimize the sums of the squares of the deviations between calculated and measured values (absolute errors).

These sums were then converted to estimates of variance by dividing by the number of degrees of freedom, in this case 100. The estimates of variance are

for j_D vs. N_{Re_3} : 0.41×10^{-6}

for j'_D vs. N_{Re_3} : 0.51×10^{-6}

At the 90% probability level the confidence ranges of these variances were as follows (*30*):

for j_D vs. N_{Re_3} : 0.33×10^{-6} to 0.53×10^{-6}

for j'_D vs. N_{Re_3} : 0.41×10^{-6} to 0.66×10^{-6}

The value of 0.51×10^{-6} for j'_D vs. N_{Re_3} lies within the confidence range of j_D vs. N_{Re_3}, so neither correlation is a significantly better fit of the data even at the 90% probability level.

In view of this inability to distinguish statistically between these two forms of correlation attention will be focused on j_D vs. N_{Re_3} because of its greater simplicity; that is, it does not require knowledge of N_{Sh_o}.

Although correlations obtained by minimizing the sums of the squares of the absolute errors can be readily compared, in many applications a more useful correlation can be obtained by minimizing the sums of the squares of the relative errors. Figure 4 indicates that the relative errors, and presumably their variance, are independent of N_{Re_3}.

A least-squares correlation was obtained for j_D vs. N_{Re_3} by minimizing the sum of the squares of the relative errors, defined as follows:

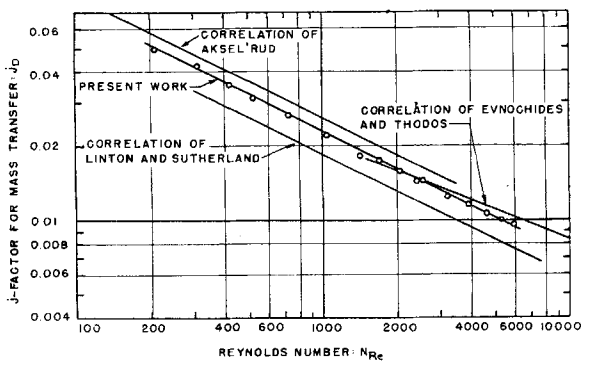

Fig. 5. Comparison of the data obtained for spheres with correlations obtained by other workers.

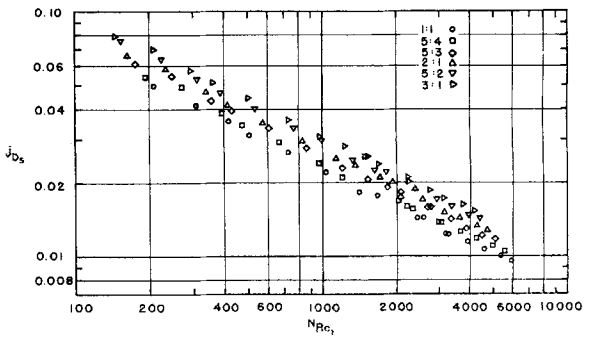

Fig. 7. Plot j_{D_s} vs. N_{Re_1}.

$$\sum_{m=1}^{m} \left(\frac{\hat{j}_{D_m} - j_{D_m}}{\hat{j}_{D_m}} \right)^2$$

The result is

$$\hat{j}_D = 0.7408\ (N_{Re_3})^{-0.501} \qquad (13)$$

The maximum deviation from Equation (13) is 5.9% .The estimated standard deviation of the data about this equation is 1.9%. The confidence limits for the constants at the 95% probability level are as follows:

for C_1 : 0.7408 ± 0.0196

for n_1 : -0.501 ± 0.004

It is of interest to note that the theoretical value for n_1 of -0.5 is included in the confidence range.

The errors involved in estimating physical properties probably preclude the use of constants with three or four significant figures. The constants were therefore rounded off within the confidence limits given above to give the expression

$$\hat{j}_D = 0.74\ (N_{Re_3})^{-0.50} \qquad (14)$$

The line representing this equation is plotted in Figure 4. The maximum deviation from Equation (14) is 6.4%, and the estimated standard deviation is 2.1%.

The present data obtained for the special case of spheres (eccentricity 1:1) can be compared with that found by other workers (*1, 5, 6, 13, 20, 27*), as shown in Figures 5 and 6. The agreement suggests that no large systematic errors were involved in the present techniques.

It is of interest to compare the data with that of Pasternak and Gauvin (*24*), obtained from spheres, hemispheres, cubes, prisms, and cylinders, the latter oriented both normal and parallel to flow. The intensity of turbulence in their work was about 10%. Their comprehensive correlation for all these shapes is

$$\hat{j}_D = 0.692\ (N_{Re_3})^{-0.486} \qquad (15)$$

This equation is also plotted on Figure 4. The maximum deviation of the present data from Equation (15) is 9.6%.

In view of the common use of D_1 with a form of k_c based on the area of a sphere of the same volume as the body it is of interest to note the level of error which this may entail in the case of spheroids, as shown by the plot of j_{D_s} vs. N_{Re_1} in Figure 7.

ACKNOWLEDGMENT

The financial support of the Shell Companies Foundation in the form of a Fellowship granted to A. R. H. Cornish is gratefully acknowledged.

NOTATION

A = surface area of spheroid
c = total concentration ($c_A + c_B$)
c_A, c_B = concentrations of components A and B
$c_{B_{1,m}}$ = log mean of the concentrations of B at the surface and at a point remote from the surface
C_1, C_2 = coefficients in Equations (2), (3), (4), and (5)
d = length of semimajor axis of an oblate spheroid
D_c = characteristic dimension representing the geometry of a body
D_v = molecular diffusivity
D_1 to D_7 = characteristic dimensions defined in text (specific forms of D_c)
f = length of semiminor axis of an oblate spheroid
g = acceleration due to gravity
$j_D, \hat{j}_D$ = experimental and calculated j factors for mass transfer, $N_{Sh}/(N_{Re})(N_{Sc})^{1/3}$
j'_D = modified j factor for mass transfer, $(N_{Sh} - N_{Sh_0})/(N_{Re})(N_{Sc})^{1/3}$
j_{D_s}, j'_{D_s} = j factors using k_c based on the area of the sphere of the same volume as the spheroid
k_c = individual continuous phase mass transfer coefficient
m_1, m_2 = exponents in Equations (2) and (3)
n_1, n_2 = exponents in Equations (4) and (5)
N'_{Gr} = Grashoff number for mass transfer, $D_c^3 g(\rho_s - \rho_\infty)/\nu^2\rho_s$
N_{Re} = Reynolds number, $D_c\ u_\infty\ \rho/\mu$
N_{Re_1} to N_{Re_7} = Reynolds numbers where D_c is replaced by D_1 to D_7, respectively
N_{Sc} = Schmidt number, $\mu/\rho\ D_v$
N_{Sh} = Sherwood number, $k_c D_c/D_v$
N_{Sh_0} = Sherwood number for transfer by purely molecular diffusion, $k_c D_c/D_v$
N = overall rate of mass transfer
P^+ = saturation vapor pressure of transferring component
P_o = partial pressure of transferring component in bulk of continuous phase
R = gas constant
T = absolute temperature
u_∞ = linear velocity

Greek Letters

μ = viscosity
ν = kinematic viscosity
ρ = density
ρ_s, ρ_∞ = continuous phase density at the body surface and in the bulk
ψ = sphericity, defined as surface area of a sphere having the same volume as the body divided by the surface area of the body

LITERATURE CITED

1. Aksel'rud, G. A., *Zhur. Fiz. Khim.*, **27**, 1445 (1953).
2. Brown, R. A. S., K. Sato, and B. H. Sage, *Chem. Eng. Data Series*, **3**, 263 (1958).
3. Bukacek, R. F., and R. E. Peck, *A.I.Ch.E. Journal*, **7**, 453 (1961).
4. Bukacek, R. F., Private communication.
5. Evnochides, Spyros, and George Thodos, *A.I.Ch.E. Journal*, **7**, 79 (1961).
6. Frössling, N., *Gerlands Beitr. Geophys.*, **52**, 170 (1938).
7. ———, *Lunds. Univ. Arsskr.*, **36**, No. 4, (1940).
8. Garner, F. H., *Trans. Inst. Chem. Engrs. (London)*, **28**, 95 (1950).
9. ———, and A. R. Hale, *Chem. Eng. Sci.*, **2**, 157 (1953).
10. Garner, F. H., and R. B. Keey, *ibid.*, **9**, 119 (1958).
11. Garner, F. H., and A. H. P. Skelland, *ibid.*, **4**, 149 (1955).
12. ———, *Ind. Eng. Chem.*, **48**, 51 (1956).
13. Garner, F. H., and R. D. Suckling, *A.I.Ch.E. Journal*, **4**, 114 (1958).
14. Gilliland, E. R., *Ind. Eng. Chem.*, **26**, 681 (1934).
15. Hughes, R. R., and E. R. Gilliland, *Chem. Eng. Progr.*, **48**, 497 (1952).
16. Keith, F. W., Jr., and A. N. Hixson, *Ind. Eng. Chem.*, **47**, 258 (1955).
17. Klee, A. J., and R. E. Treybal, *A.I.Ch.E. Journal*, **2**, 444 (1956).
18. Lewis, J. B., I. Jones, and H. R. C. Pratt, *Trans. Inst. Chem. Engrs. (London)*, **29**, 126 (1951).
19. Linton, W. H., Jr., and T. K. Sherwood, *Chem. Eng. Progr.*, **46**, 258 (1950).
20. Linton, M., and K. L. Sutherland, *Chem. Eng. Sci.*, **12**, 214 (1960).
21. Maisel, D. S., and T. K. Sherwood, *Chem. Eng. Progr.*, **46**, 131, 172 (1950).
22. Malaika, J., Ph.D. thesis, State University of Iowa, Iowa City, Iowa (1949).
23. Mueller, M. W., and R. E. Peck, *Ind. Eng. Chem. Anal. Ed.*, **15**, 46 (1943).
24. Pasternak, I. S., and W. H. Gauvin, *Can. J. Chem. Engr.*, **38**, 35 (April, 1960).
25. Perry, John H., ed., "Chemical Engineers' Handbook," 3 ed., p. 1018, McGraw-Hill, New York (1950).
26. *Ibid.*, p. 370.
27. Ranz, W. E., and W. R. Marshall, *Chem. Eng. Progr.*, **48**, 141, 173 (1952).
28. Steinberger, R. L., and R. E. Treybal, *A.I.Ch.E. Journal*, **6**, 227 (1960).
29. Uno, S., Ph.D. thesis, Ill. Inst. Technol., Chicago, Illinois (1958).
30. Volk, W., "Applied Statistics for Engineers," p. 152, McGraw-Hill, New York (1958).
31. Williams, G. C., Sc.D thesis, Mass. Inst. Technol., Cambridge, Massachusetts (1942).
32. Skelland, A. H. P., and R. H. Cornish, to be published.

Manuscript received January 15, 1962; revision received June 8, 1962; paper accepted June 11, 1962. Paper presented at A.I.Ch.E. Los Angeles meeting.